Heliyon 10 (2024) e25516

Contents lists available at ScienceDirect

Heliyon

journal homepage: www.cell.com/heliyon

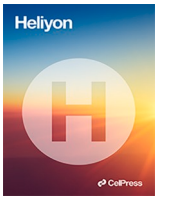

Research article

Characterization of nanoscale atomic motion of Si in polycrystalline Cu layer

Viktor Takáts [a], Eszter Bodnár [a,c], Yuri Kaganovskii [b], Tamás Fodor [a], József Hakl [a], Sándor Molnár [a], Márton Soha [a], Kálmán Vad [a,*]

[a] Institute for Nuclear Research, H-4026 Debrecen, Bem Tér 18/C, Hungary
[b] Department of Physics, Bar-Ilan University, Ramat-Gan 52900, Israel
[c] University of Debrecen, Doctoral School of Physics, 4032 Debrecen, Egyetem Tér 1, Hungary

ARTICLE INFO

Keywords:
Nanocrystalline Cu
Cu/Si nanolayers
Grain boundary diffusion
Nanoscale diffusion
Low energy ion scattering

ABSTRACT

Atomic migration of silicon through grain boundaries of a thin polycrystalline Cu film and island formation on the Cu surface were studied in the temperature range of 403–520 K. Samples used in these experiments was prepared on Si(111) wafers by room temperature magnetron sputtering and they consisted of amorphous Si layer (80 nm) and polycrystalline Cu layer (40 nm). The silicon layer served as the source layer of diffusion, while the copper surface was the accumulation surface. Detection of Si atoms on the accumulation surface after penetration through the Cu layer was made by low energy ion scattering spectroscopy and the grain boundary diffusion coefficient D_{GB} was determined from the appearance time. The depth distribution of Si in the Cu film was analysed by secondary neutral mass spectroscopy. From this depth distribution, D_{GB} was also determined. By scanning probe microscope and electron microscope measurements, it was experimentally detected that Si atoms on the Cu surface did not form a continuous layer. Instead, amorphous Si islands were formed at the accumulation surface with surface protrusions in their centres.

1. Introduction

For production of sub-micron size electronic devices on Si wafers, microelectronic industry uses Cu as on-chip conductors. Due to miniaturization, problems of reliability require a detailed examination of nanoscale atomic mixing between Cu and Si. Since working temperature of an electronic circuit is usually higher than the room temperature, there is an opportunity for atomic mixing due to grain boundary (GB) diffusion of Si through the Cu layer, followed by accumulation on the Cu surface. Despite the fundamentals of GB diffusion which are at present well elaborated and outlined [1–5], the surface segregation factors (σ) have not been measured yet. Segregation denotes the enrichment of a constituent at the free surface and modifies the macroscopic properties of materials, so its study is important from the points of physics and technical application. According to the surface accumulation method developed by Hwang and Balluffi and applied for study of GB diffusion [6,7], one can only determine the ratio of D_{GB}/σ (D_{GB} is the GB diffusion coefficient) instead of directly determining D_{GB}.

In this paper we report on the results of nanoscale measurements of silicon diffusion through a polycrystalline copper layer in pure C-type diffusion kinetic regime, according to Harrison's classification [8], and on the results of direct determination of Si segregation

* Corresponding author.
E-mail address: vad@atomki.hu (K. Vad).

https://doi.org/10.1016/j.heliyon.2024.e25516
Received 19 October 2023; Received in revised form 23 January 2024; Accepted 29 January 2024
Available online 1 February 2024

factor σ on the Cu surface. In our experiments we used the Low Energy Ion Scattering (LEIS) spectroscopy [9]. LEIS is especially suitable for studying surface segregation phenomena because the information depth is lower than 1 nm, in contrast to the few nanometres of the Auger electron spectroscopy or the few micrometers of the radiotracer method [10,11]. We managed to determine D_{GB} from the time t_0 during which the Si atoms diffuse through a Cu layer and reach the surface, and from the depth distribution of Si in the Cu layer. It turned out from the exploration of the surface accumulation mechanism of Si that silicon forms atomic islands on the Cu surface instead of a thin continuous layer as it was formerly supposed by Hwang and Balluffi model [6,7]. From the size distribution analysis of islands, an exponential decrease in the number of islands was experienced with the increase in the size of islands.

2. Experiments

2.1. Sample preparation and experimental arrangements

Samples were prepared by successive magnetron sputtering of amorphous Si layer (about 80 nm thickness) and polycrystalline Cu film (40 nm thickness) onto (111) Si-wafer at room temperature (Cu(40 nm)/Si(80 nm)//Si). After preparation, the samples were placed into a high vacuum chamber with a base pressure of 10^{-10} mbar for low energy ion scattering spectroscopy measurements. LEIS is a surface sensitive method that enables the composition analysis of the few top-most surface atomic layers. Study of atomic diffusion by LEIS was first achieved by the authors of the paper [12]. In the present experiments, a helium ion beam of 1 keV/10 nA was used to scan sample surfaces. During measurements, the maximum pressure in the LEIS chamber was 10^{-7} mbar due to the He gas inflow. Samples were annealed at different temperatures between 403 K and 520 K for various annealing times. A tungsten hot plate was used for sample heating. The temperature was controlled with a Eurotherm temperature controller and was measured with a pyrometer focused on the sample holder surface. This solution made it possible to avoid the interfering effect of sample surface brightness. Prior to annealing, the emissivity coefficient of the sample holder, which is essential to correct temperature measurements, was determined by comparison of the temperatures measured by radiation and thermocouple.

The sensitivity of LEIS increases with the increase in ion energy and beam intensity. In this case, however, the surface sputtering rate also increases together with the distortion of surface composition. In order to avoid this problem, in our experiment a low energy ^{4}He ion beam (1 keV) was used for surface irradiation. The sputtering effect was checked by a separate measurement. We received the value of 5×10^{-4} nm/s for the ion etching rate. The effect of this low-rate etching was further restricted. The ion beam was blanked by an electrostatic beam blanker while the sample was rotated on its axis. The beam was focused into a 3 mm diameter spot with 2–3 mm offset from the axis. In this way, by rotation of the sample, each LEIS measurement could be performed on a fresh surface area of the sample, enabling us to avoid the ion etching effect during longer measurements.

At successive stages of the experimental procedure, we checked the film structure by two methods. First, the surface morphology change of samples during annealing was analysed by an atomic force microscope (AFM). Secondly, samples were investigated by a secondary neutral mass spectrometer (SNMS) to reveal the Si and Cu depth distributions in the layered structure before and after annealing. The working principle of SNMS is similar to that of secondary ion mass spectrometer (SIMS). In both cases the sample surface is sputtered by an ion beam, whereupon secondary ions and secondary neutral particles leave the surface. While the secondary ions are analysed by a mass spectrometer in SIMS, in SNMS the neutral particles are analysed [13,14]. In SNMS, the ion beam consists of Ar^+ ions extracted from an Ar plasma and it is used for sputtering through a Ta mask with 2 mm hole in the centre. The great advantage of SNMS is that the sputtering energy (Ar^+ ion energy) can be rather small, a few hundred eV, whereby the surface atomic mixing evoked by the ion scattering can be confined to 1 nm thick surface layer. Since the atomic mixing is a disturbing effect in sputter-based depth profile analyses, the application of SNMS for nanometer scale depth profile analyses seems to be an excellent solution [15] although concentrations of chemical components appertain to a macroscopic surface area (average concentrations are measured). In present experiments the kinetic energy of Ar^+ ions was set to 350 eV.

Surface analysis was also made by backscattered electron imaging. It is well-known that some part of the electron beam in an electron microscope is reflected back from the sample surface after elastic interactions between the beam and the sample. These electrons are called backscattered electrons. The intensity of backscattered electrons is sensitive to the atomic number of the atoms on which the electrons are scattered. The higher the atomic number, the brighter the appearance of the material in the image. In the present work, this quality was very useful because it allowed us to make maps of the lateral atomic arrangement on the surfaces.

Finally, X-ray diffraction (XRD) measurements were performed for the phase identification of crystal structures.

2.2. Depth profile analysis

Study of nanoscale physical processes requires a precise depth profile analysis technique. The aim of depth profiling is to reveal the in-depth chemical composition of a surface layer. In order to reach this aim, depth profile techniques are based on surface sputtering in general. Depth profiles obtained by sputtering differ from the real in-depth distributions due to sputter-induced changes in surface composition and topography. Thus, a critical interpretation of experimental results obtained by sputtering is needed to receive the real depth distributions of constituents.

Chemical components of a sharp interface can be mixed by sputtering even if they were not mixed initially. Ion scattering on interface atoms, surface roughness, and crater shape (crater formation is inherent in sputtering) can bring about some mixing among interface atoms and the depth resolution fails [16–18]. The ion scattering can be neglected by using low (a few hundred eV) kinetic energy ions for sputtering. In this case, the depth resolution is essentially defined by the surface roughness and crater shape. The surface roughness characterizes the surface shape by deviations of the real surface from its ideal form in the normal vector direction of

the surface. The contribution of the surface roughness can be taken into consideration by a Gaussian type distribution of surface shape deviations [16]. The best depth resolution is achieved when the crater bottom is flat and has small surface roughness.

In order to get information about the real atomic mixing at an interface, we calculated the depth distribution of constituents in addition to experimental measurements with the assumption that the interface is ideal. An interface between two layers is ideal if there is no atomic mixing between the layers. The working principle of calculation starts with the definition of a calculation volume. For example, it can be 1 nm thick layer. The next step in the calculation procedure is the determination of yields of composition elements found in this calculation volume. Finally, the whole interface is scanned by this calculation volume in the direction perpendicular to the sample surface which results in the depth profiles of composition elements.

The surface roughness and crater shape can be experimentally measured by a profilometer. The advantage of using a profilometer is that the surface roughness is defined on the same macroscopic scale where the SNMS depth profiling is done. This surface roughness value is larger than it would be measured on the nanoscale. The measured surface roughness and crater shape are used in the calculation as input parameters. Comparison between the calculated and measured profiles gives information about the real depth distributions of atomic components. If the calculated depth distribution fits well with the experimental data, the measured depth distribution is only determined by sputtering, if not, the difference between the measured and calculated values is determined by other physical processes, like atomic mixing during sample preparation or diffusion [19].

2.3. Calculation of D_{GB}

Calculations of GB diffusion coefficients were done in two different ways. In the first one, the appearance time t_0 was used to calculate it. The appearance time is the time when silicon atoms first appear on the copper layer surface during annealing. Since in our experiments pure C-type GB diffusion was realized, the function of Si concentration in copper GBs (denoted by C_{GB}) follows the well-known complementary error function [20]:

$$C_{GB}(y) = C_0 \bullet erfc\left(\frac{y}{2\sqrt{D_{GB}t}}\right). \tag{1}$$

Here y is the length parameter in GBs and varies from the diffusion source ($y = 0$) to the top ($y = h$) of the film, D_{GB} is the GB diffusion coefficient of Si in polycrystalline copper, C_0 is the concentration of Si atoms at the source surface, t is the diffusion time. If Si atoms diffuse through the Cu film and reach its surface in the time of t_0, we can write that

$$\frac{C_{GB}(h)}{C_0} = erfc\left(\frac{h}{2\sqrt{D_{GB}t_0}}\right), \tag{2}$$

where $C_{GB}(h)$ is the diffusant (Si) concentration inside the copper film at $y = h$ position. The concentration ratio *of* $C_{GB}(h)/C_0$ can be determined from the depth distribution of Si in the Cu layer measured by SNMS depth profiling. According to Eq. (2), this ratio equals erfc (Z), where $Z = \frac{h}{2\sqrt{D_{GB}t_0}}$. The diffusion distance which is equal to the film thickness h and the diffusion time which is equal to the appearance time t_0 are measured experimentally, thus from Eq. (2) the GB diffusion coefficient can be obtained.

GB diffusion coefficients can also be calculated from the depth distribution of diffusant atoms along grain boundaries. From Eq. (1) one can obtain another relation, namely,

$$\frac{\partial C_{GB}(y)}{\partial y} = -\frac{C_0}{\sqrt{\pi D_{GB}t}} exp\left(-\frac{y^2}{4D_{GB}t}\right). \tag{3}$$

The minus sign on the right side of this equation denotes that the concentration of diffusant decreases with diffusion length (y). If the concentration distribution $C_{GB}(y)$ is experimentally measured as a function of diffusion length and the measured data are plotted in

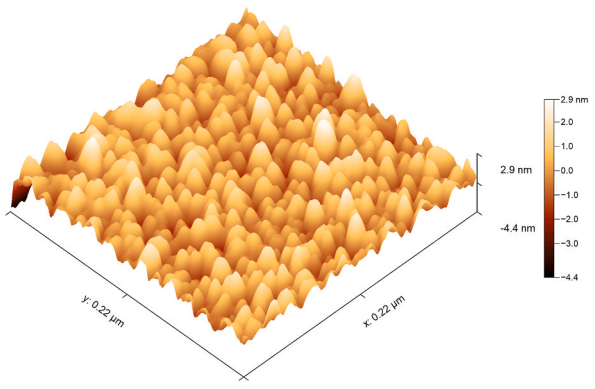

Fig. 1. Grain structure of the polycrystalline Cu film used in our measurements.

the form of $ln\left(\frac{\partial C_{GB}}{\partial y}\right)$ *vs.* y^2, the linear fit of the received data yields a slope which is inversely proportional to the GB diffusion coefficient.

3. Results and discussion

3.1. Sample characterization

An AFM image of an as-prepared sample surface is shown in Fig. 1. The copper layer had a polycrystalline structure with uniform grain distribution. The maximum grain diameter was about 15 nm which was checked by XRD measurements as well. As it can be seen, the surface was not smooth at the nanoscale, it had a surface roughness with 7,3 nm peak-to-valley value which is a very important characteristic from the point of surface diffusion.

3.2. Determination of D_{GB} from appearance time and depth distribution

As it was mentioned previously, in our experiments D_{GB} could be calculated by Eq. (2) using the experimentally measured values of t_0 and $C_{GB}(h)/C_0$. The appearance time t_0 was determined from the time dependence of Si LEIS peak by extrapolating its height to zero (see Ref. [21]). We found in LEIS measurements that the detection sensitivity of Si is about 0.1 % of a monolayer ($\sim 10^{12}$ atoms/cm^2). The ratio $C_{GB}(h)/C_0$ was calculated from concentration depth distributions of Si atoms along copper GBs (Fig. 2). The value $C_{GB}(h)$ can be clearly defined by point (b) in this curve. However, the determination of Si concentration at the source surface C_0 was a little more complicated on the depth scale. In the model of Hwang and Balluffi [6,7], the source surface is the surface where diffusant atoms enter the grain boundary channels. In our layered structure this is the Cu/Si interface. The question arises, how we can define this interface on the depth scale. In Fig. 2, the Si depth distributions measured experimentally (blue symbols) and the calculated Si depth distribution (red line) are presented. It can be seen that the experimentally measured values start to differ from the calculated one at the point (a) if the depth decreases.

In the case of the as-deposited sample (blue open symbols), the difference indicates an atomic mixing between Cu and Si during sample preparation. The same type atomic mixing was also experienced at the interfaces of Cu/Si bilayer samples prepared by magnetron sputtering [22]. The explanation of this phenomenon was 1) high porosity of thin layers owing to high kinetic energy of deposited particles 2) an increase in the substrate temperature when the sample was exposed to the heating effect of the plasma during preparation. Due to the high layer porosity and the enhanced substrate temperature, the silicon diffusivity and so the atomic mixing had increased. The atomic mixing produced by the preparation technique does not affect the Si GB diffusion process because the Si concentration in the Cu layer is small and Si is not concentrated in GBs.

In the case of the annealed sample (blue filled symbols), the difference is even higher than that of the as-deposited sample and is the result of diffusion. The surface at the point (a) on the depth scale is the source surface since the GB diffusion starts here. Hereupon, the ratio $C_{GB}(h)/C_0$ can be defined from the two concentration values and, with the measured appearance time t_0, the grain boundary diffusion coefficient D_{GB} can be calculated. The Si concentration at the point (a) is about 20 % (Fig. 2). The ratio of the grain boundary surface to the total layer surface is also near 20 % as it can be determined by analysis of AFM pictures, i.e., the grain boundary channels are entirely filled up with Si atoms at the source surface.

Inside grain boundaries, the Si concentration drops gradually from the initial value to $C_{GB}(h) \approx 1.5$ % (which is the Si concentration near the accumulation surface) and increases again at the Cu surface due to surface segregation. The concentration of Si atoms on the copper surface is $C_S \approx 10$ % and thus the surface segregation factor $\sigma = C_S/C_{GB}(h)$ can be calculated. For the Si segregation factor in Cu at 453 K, we received the value of $\sigma \approx 7$. In the Cu intensity there is a slight local minimum at 10 nm depth (Fig. 2). The explanation is that after LEIS measurements, prior the depth profile analysis, a Cu layer was deposited on the sample surface as a cap layer. The necessity of this extra layer was motivated by the working principle of SNMS where the emission and ionization of particles are made

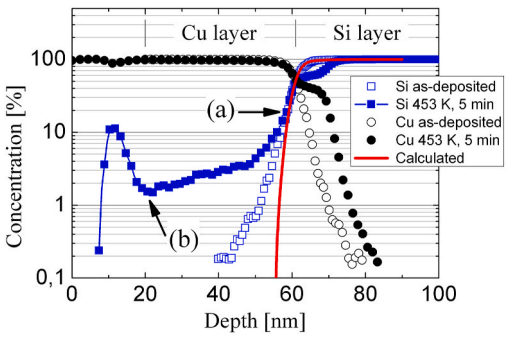

Fig. 2. Depth distributions of Cu and Si in a Cu(40 nm)/Si(80 nm) bilayer before and after annealing at 453 K for 5 min. Symbols are the experimental values measured by SNMS. The red line is the calculated concentration distribution of Si. (For interpretation of the references to colour in this figure legend, the reader is referred to the Web version of this article.)

with a radiofrequency plasma and, at the start of sputtering, the process needs some time to stabilize. The lack of this cap layer is not a problem if the effective thickness of the diffusant Si layer on the Cu surface is high, but if it is low, the correct Si intensity cannot be achieved.

Temperature dependence of the GB diffusion coefficient derived from the appearance time t_0 is presented with open symbols in Fig. 3 (see also Fig. 4 of the paper [21]). From the penetration profiles of Si atoms obtained by SNMS, $ln\left(\frac{\partial C_{GB}}{\partial y}\right)$ could be calculated as a function of y^2, where y is the diffusion length according to the Chapter 2.3. The experimental values and their linear fit are shown in Fig. 4. For the diffusion time in Eq. (3) we chose the appearance time ($t = t_0$) because the final concentration distribution evolved in the GBs during the appearing time and it did not change further on. The results are plotted in Fig. 3 with solid squares. As it can be seen, the diffusion coefficients calculated from the penetration profile were approximately the same as calculated from the appearance times, i.e., the two methods provided nearly the same results.

The measurements were performed in the temperature range of the C-type diffusion kinetic regime. At the highest temperature (453 K), the measured values were higher than the linear fits in both methods, reflecting an increase in the effective activation energy. The possible increase in the activation energy with temperature was previously discussed in the paper of Hwang and Balluffi [23]. It is obvious that polycrystalline thin films contain several types of GBs and each of them is characterized by different activation energy Q_{GB}. The observed activation energy for GB diffusion is therefore a weighted average of the various Q_{GB}. At low temperatures the diffusion which has the smallest Q_{GB} occurs along GBs, at higher temperatures the GBs with higher Q_{GB} will be involved in the total diffusion process.

In Fig. 2, both Si and Cu concentrations of annealed samples show a step-like drop between the depths of 60 and 70 nm (solid symbols). Atomic diffusion at the interface could not cause this effect because the character of Cu concentration distribution did not change due to annealing. We believe that the origin of the step-like concentration drop could be a phase change in the crystal structure at the interface. Due to annealing, a chemical reaction took place between Cu and Si atoms and a new phase Cu_xSi_y was formed. This solid phase evoked a change in the detection sensitivity factor of Si during depth profiling which is reflected in the concentration drop. According to Moiseenko et al. [24], the reaction in nanolayers between Cu and Si is initiated at about 400 K and occurs in three steps: formation of amorphous CuSi phase, then formation of clusters Cu_3Si and, finally, formation of the η''-Cu_3Si phase. The step-like drop of Si concentration seen in Fig. 2 is about 50 %. The phase formation was checked by an XRD measurement on a separate sample. For this measurement, the annealing temperature was also 453 K but the annealing time was longer than 5 min so as to increase the thickness of the Cu_3Si phase which allowed us to record the diffractogram and identify the crystal phase (Fig. 5).

3.3. Si islands on Cu surface

Continuation of annealing after Si atoms appeared on the surface induced significant changes in the surface morphology. The initially uniform grain distribution (Fig. 1) became uneven. The grain symmetry decreased (skewness parameter increased) and the peakedness of grains increased (kurtosis parameter increased). Silicon protrusions were formed on the accumulation surface due to diffusion (spike-like formations in Fig. 6). These protrusions were surrounded by deeper surface parts and, in this way, these arrangements can be considered as Si islands.

In the present work, we measured the Si content of the sample surface by LEIS. The Si peak area in a LEIS spectrum is proportional to the Si content of the surface, i.e., to the surface coverage. Consequently, time evolution of the Si peak in a LEIS spectrum gives information on time evolution of the surface coverage during annealing. Fig. 7 shows that the coverage increased with the annealing time and approached to a saturation value which is near 30 % of the total accumulation surface. The times when these curves intersect the time axis are the appearance times. Saturation of surface coverage was a consequence of diffusion mechanism. The atomic flux through the copper layer continuously decreased with time and finally halted. This saturation effect of surface coverage was also experienced previously in Ni/Cu bilayer systems by Cu diffusion through a Ni layer [12], suggesting that this is a general effect in thin layers.

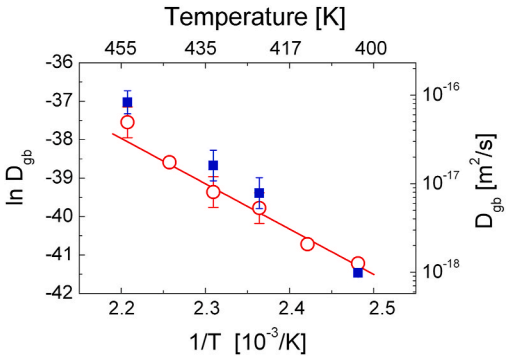

Fig. 3. Temperature dependence of Si grain boundary diffusion coefficient D_{gb} in copper nanocrystalline layer. The open symbols were calculated from the appearance time [21], the solid squares were calculated from the concentration slopes of Si inside grain boundaries.

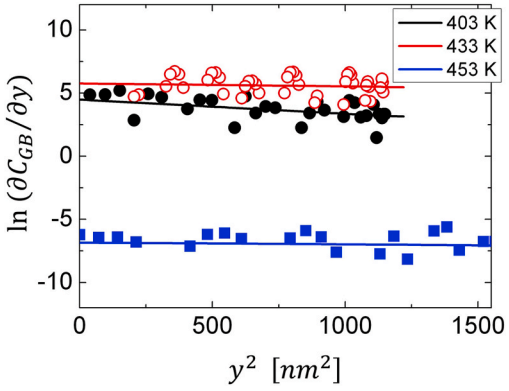

Fig. 4. Plots of $ln\left(\frac{\partial C_{GB}}{\partial y}\right)$ *vs.* y^2 measured at different temperatures.

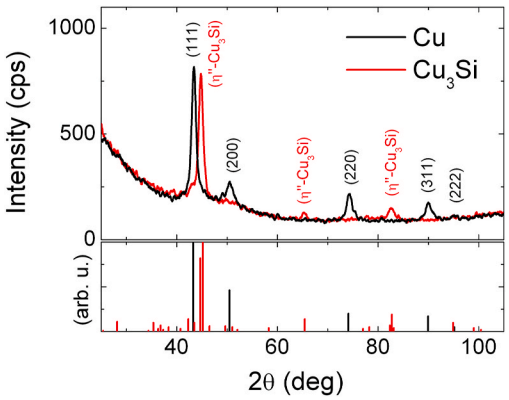

Fig. 5. XRD diffractograms of a Cu(40 nm)/Si(80 nm) bilayer sample before (black curve) and after (red curve) annealing at 453 K for 2 h. The peaks of the black curve correspond to the crystal structure of Cu, while the peaks of the red curve correspond to the η'' phase of Cu_3Si. The bottom part of the diffractogram shows the reference positions of Cu and Cu_3Si peaks according to the datasheets 00-004-0836 and 00-059-0263 of ICDD database. (For interpretation of the references to colour in this figure legend, the reader is referred to the Web version of this article.)

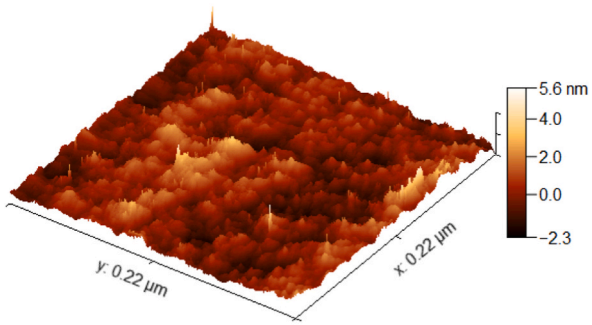

Fig. 6. AFM picture of the grain structure of the polycrystalline Cu film surface after the sample was annealed at 480 K for 8 min. The spike-like protrusions on the surface are the consequence of Si diffusion. Due to annealing the skewness parameter increased from 0,09 to 0,47 and the kurtosis parameter also increased from 0,27 to 0,52.

Near the saturation state, the sample surface was scanned by AFM again. Fig. 8 shows the result when the sample was annealed at 520 K for 10 min. The increase in Si concentration of the surface resulted in an increase in the number of Si islands and, as it can be seen, the surface morphology changed significantly. According to the AFM measurements, the height of the evolved surface protrusions was about 5–6 nm.

The Si islands evolved on the Cu surface were investigated by electron microscope, too. Silicon on Cu background could be well studied by back scattered electrons due to the difference between atomic numbers. In the microscope images made with back scattered

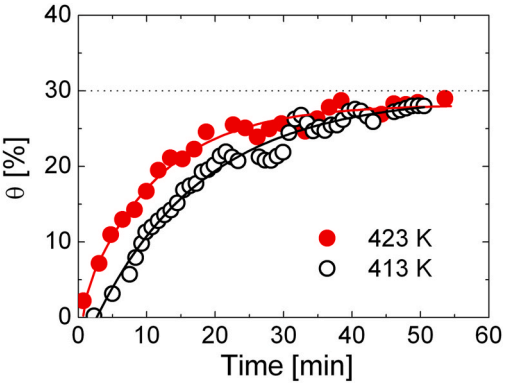

Fig. 7. Surface coverage (Θ) of Cu(40 nm)/Si(80 nm)//Si samples by silicon atoms as a function of annealing time. The coverage approaches to a saturation value of about 30 % of the total surface. The samples were annealed at 413 K and 423 K. (For interpretation of the references to colour in this figure legend, the reader is referred to the Web version of this article.)

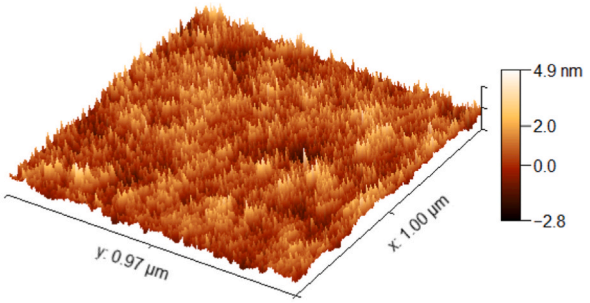

Fig. 8. AFM picture of the Cu film surface after the sample was annealed at 520 K for 10 min. The number of spike-like Si protrusions on the surface increased drastically.

electrons, Si islands look like grey spots (Fig. 9). The darkness of a spot depends on the Si concentration. The darker grey spots inside amorphous Si islands are Si nuclei which form the spike-like surface protrusions. Si islands and protrusions are sinks for Si atoms diffusing through GBs of Cu layer.

We evaluated the blackness distribution of microscope images by mean-grey-value analysis and could determine both the surface Si coverage and the size distribution of Si spots (islands). For Si coverage we obtained 32 % of the total surface area which is close to the saturation value obtained by LEIS (Fig. 7). The size distribution of Si islands was plotted in the coordinate system of ln*(N) vs. d*, where *d* is the island diameter and *N* is the number of Si islands with diameter of *d* (Fig. 10). As it can be seen, the number *N* decreased

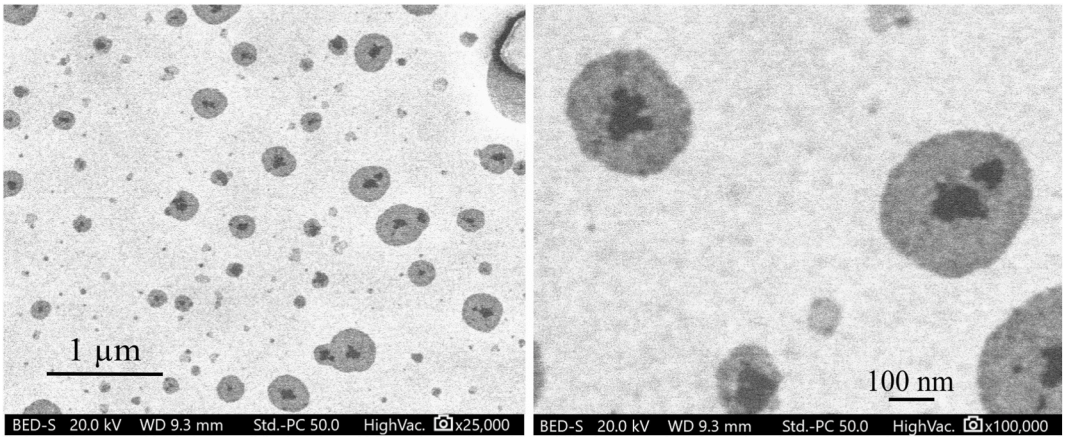

Fig. 9. Electron microscope images of the sample surface annealed at 423 K for 30 min. Grey spots are the Si islands, the light part of the surface is Cu. Darker spots inside the islands are crystalline nuclei.

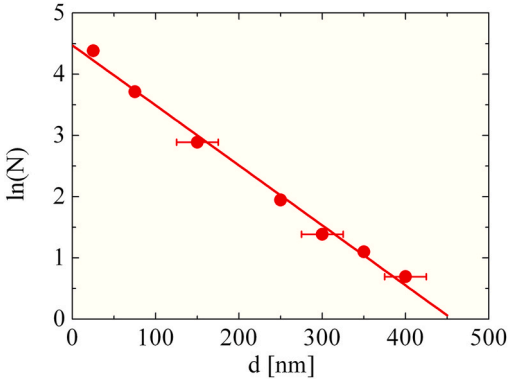

Fig. 10. Size distribution of Si islands on the Cu surface. N and *d* denote the number and diameter of islands.

exponentially with the increase in diameter and the maximum diameter of Si islands which could be achieved by GB diffusion is about 450 nm. The diffusion flux stopped before the islands could grow further.

4. Conclusions

A study of nanoscale atomic motion in thin film structures requires a precise depth profile analysis technique. In the present work we studied the Si depth distribution in Cu polycrystalline layers as a result of GB diffusion. The atomic motion was induced by low temperature thermal annealing. The diffusion coefficient was calculated from both the appearance time and the concentration gradient of Si inside GBs. The segregation factor of Si in polycrystalline copper was defined by concentration of Si on the accumulation surface of a Cu/Si//Si bilayer structure. The silicon concentration on the sample surface was studied by LEIS. The surface coverage had a saturation character as a function of annealing time. The surface morphology changed significantly by annealing. It was confirmed that, at temperatures of the C-type diffusion kinetic regime, Si islands evolved on the surface instead of a continuous layer, as it was previously assumed in other papers [25–27]. The island structure was studied by electron microscopy.

Data availability statement

No data was used for the research described herein.

CRediT authorship contribution statement

Viktor Takáts: Supervision, Investigation, Conceptualization. **Eszter Bodnár:** Methodology, Investigation, Data curation. **Yuri Kaganovskii:** Writing – original draft, Validation, Conceptualization. **Tamás Fodor:** Investigation, Data curation. **József Hakl:** Validation, Methodology, Investigation. **Sándor Molnár:** Investigation, Data curation. **Márton Soha:** Investigation, Data curation. **Kálmán Vad:** Writing – review & editing, Validation, Methodology, Conceptualization.

Declaration of competing interest

The authors declare that they have no known competing financial interests or personal relationships that could have appeared to influence the work reported in this paper.

Acknowledgements

This work was carried out in the frame of the projects TKP2021-NKTA-42 and 2019–2.1.7-ERANET-2021-00021 financed by the National Research, Development and Innovation Fund of the Ministry for Innovation and Technology, Hungary.

References

[1] I. Kaur, W. Gust, L. Kozma, Handbook of Grain and Interphase Boundary Diffusion Data, Ziegler Press, Stuttgart, 1989.
[2] I. Kaur, Y. Mishin, W. Gust, Fundamentals of Grain and Interphase Boundary Diffusion, Wiley & Sons LTD, Chichester, New York, 1995.
[3] Y. Mishin, Chr Herzig, J. Bernardini, W. Gust, Grain boundary diffusion: fundamentals to recent developments, Int. Mater. Rev. 42 (1997) 155–178, https://doi.org/10.1179/IMR.1997.42.4.155.
[4] Y. Mishin, Chr. Herzig, Grain boundary diffusion: recent progress and future research, Mater. Sci. Eng., A 260 (1999) 55–71, https://doi.org/10.1016/S0921-5093(98)00978-2.
[5] Chr Herzig, S.V. Divinski, Grain boundary diffusion in metals: recent development, Mater. Trans. 44 (2003) 14–27, https://doi.org/10.2320/matertrans.44.14.
[6] J.C.M. Hwang, R.W. Balluffi, Measurement of grain-boundary diffusion at low temperatures by the surface accumulation method. I. Method and analysis, J. Appl. Phys. 50 (1979) 1339–1348, https://doi.org/10.1063/1.326168.

[7] J.C.M. Hwang, J.D. Pan, R.W. Balluffi, Measurement of grain boundary diffusion at low temperature by the surface accumulation method. II. Results for goldsilver system, J. Appl. Phys. 50 (1979) 1349–1359, https://doi.org/10.1063/1.326115.
[8] L.G. Harrison, Influence of dislocations on diffusion kinetics in solids with particular reference to the alkali halides, Trans. Faraday Soc. 57 (1961) 1191–1199, https://doi.org/10.1039/TF9615701191.
[9] H.H. Brongersma, M. Draxler, M. de Ridder, P. Bauer, Surface composition analysis by low-energy ion scattering, Surf. Sci. Rep. 62 (2007) 63–109, https://doi.org/10.1016/j.surfrep.2006.12.002.
[10] S. Divinski, J. Ribbe, G. Schmitz, C. Herzig, Grain boundary diffusion and segregation of Ni in Cu, Acta Mater. 55 (2007) 3337–3346, https://doi.org/10.1016/j.actamat.2007.01.032.
[11] D. Prokoshkina, V.A. Esin, G. Wilde, S.V. Divinski, Acta Mater. 61 (2013) 5188–5197, https://doi.org/10.1016/j.actamat.2013.05.010.
[12] V. Takáts, A. Csík, J. Hakl, K. Vad, Diffusion induced atomic islands on the surface of Ni/Cu nanolayers, Appl. Surf. Sci. 440 (2018) 275–281, https://doi.org/10.1016/j.apsusc.2018.01.087.
[13] H. Oechsner, L. Reichert, Energies of neutral sputtered particles, Phys. Lett. 23 (1966) 90–92.
[14] K. Vad, A. Csik, G.A. Langer, A. Secondary neutral mass spectrometry – a powerful technique for quantitative elemental and depth profiling analyses of nanostructures, Spectrosc. Eur. 21 (2009) 13–16.
[15] D.L. Beke, Yu Kaganovskii, G.L. Katona, Interdiffusion along grain boundaries – diffusion induced grain boundary migration, low temperature homogenization and reactions in nanostructured thin films, Prog. Mater. Sci. 98 (2018) 625–674, https://doi.org/10.1016/j.pmatsci.2018.07.001.
[16] S. Hofmann, Sputter depth profile analysis of interfaces, Rep. Prog. Phys. 61 (1998) 827–888, https://doi.org/10.1088/0034-4885/61/7/002. Reports on Progress in Physics 61 (1998), 827-888.
[17] S. Hofmann, From depth resolution to depth resolution function: refinement of the concept for delta layers, single layers and multilayers, Surf. Interface Anal. 27 (1999) 825–834, https://doi.org/10.1002/(SICI)1096-9918 (199909)27:9<825::AID-SIA638>3.0.CO;2-D.
[18] S. Hofmann, Ultimate depth resolution and profile reconstruction in sputter profiling with AES and SIMS, Surf. Interface Anal. 30 (2000) 228–236, https://doi.org/10.1002/1096-9918 (200008)30:1<228::AID-SIA821>3.0.CO;2-E.
[19] P. Joice Sophia, G. Attolini, M. Bosi, E. Buffagni, C. Ferrari, C. Frigeri, K. Vad, A. Csik, V. Takáts, Z. Zolnai, Influence of surface roughness on interdiffusion processes in InGaP/Ge heteroepitaxial thin films, ECS Journal of Solid State Science and Technology 4 (2015) P53–P56, https://doi.org/10.1149/2.0021503jss.
[20] J. Crank, The Mathematics of Diffusion, Clarendon Press, Oxford, 1975, p. 21.
[21] E. Bodnár, V. Takáts, T. Fodor, J. Hakl, Y. Kaganovskii, G. Yang, X. Yaod, K. Vad, Grain boundary diffusion of Si in polycrystalline copper film, Vacuum 203 (2022) 111260, https://doi.org/10.1016/j.vacuum.2022.111260.
[22] A.M. Ektessabi, Temperature dependence of atomic mixing at the copper-silicon interface, Thin Solid Films 236 (1993) 135–139, https://doi.org/10.1016/0040-6090(93)90658-C.
[23] J.C.M. Hwang, R.W. Balluffi, On a possible temperature dependence of the activation energy for grain boundary diffusion in metals, Scripta Metall. 12 (1978) 709–714, https://doi.org/10.1016/0036-9748(78)90313-7.
[24] E.T. Moiseenko, V.V. Yumashev, R.R. Altunin, G.M. Zeer, N.S. Nikolaeva, O.V. Belousov, S.M. Zharkov, Solid-state reaction in Cu/a-Si nanolayers: a comparative study of STA and electron diffraction data, Materials 15 (2022) 8457, https://doi.org/10.3390/ma15238457.
[25] Z. Balogh, Z. Erdélyi, D.L. Beke, A. Portavoce, Ch Girardeaux, J. Bernardini, A. Rolland, Determination of grain boundary diffusion coefficients in C-regime by hwang-balluffi method: silver diffusion in Pd, Defect Diffusion Forum (2009) 763–767, https://doi.org/10.4028/www.scientific.net/DDF.289-292.763, 289-292.
[26] Z. Bastl, J. Zidu, K. Rohacek, Determination of the diffusion coefficient of aluminium along the grain boundaries of gold films by the surface accumulation method, Thin Solid Films 213 (1992) 103–108, https://doi.org/10.1016/0040-6090(92)90482-Q.
[27] Z. Erdélyi, Ch Girardeaux, G. Langer, L. Daróczi, A. Rolland, D. Beke, Determination of grain-boundary diffusion coefficients by Auger electron spectroscopy, Appl. Surf. Sci. (2000) 213–218, https://doi.org/10.1016/S0169-4332(00)00194-X, 162–163.